

High-temperature signatures of quantum criticality in heavy fermion systems

J. Kroha¹, M. Klein², A. Nuber², F. Reinert^{2,3},
O. Stockert⁴ and H. v. Löhneysen^{5,6}

¹ Physikalisches Institut and Bethe Center for Theoretical Physics,
Universität Bonn, Nussallee 12, 53115 Bonn, Germany
E-mail: kroha@physik.uni-bonn.de

² Universität Würzburg, Experimentelle Physik II, Am Hubland,
97074 Würzburg, Germany

³ Forschungszentrum Karlsruhe, Gemeinschaftslabor für Nanoanalytik,
76021 Karlsruhe, Germany

⁴ Max Planck Institute for Chemical Physics of Solids, Nöthnitzer Str. 40,
01187 Dresden, Germany

⁵ Physikalisches Institut, Universität Karlsruhe, 76128 Karlsruhe, Germany

⁶ Forschungszentrum Karlsruhe, Institut für Festkörperphysik, 76021 Karlsruhe,
Germany

Abstract. We propose a new criterion for distinguishing the Hertz-Millis (HM) and the local quantum critical (LQC) mechanism in heavy fermion systems with a magnetic quantum phase transition (QPT). The criterion is based on our finding that the spin screening of Kondo ions can be completely suppressed by the RKKY coupling to the surrounding magnetic ions even without magnetic ordering and that, consequently, the signature of this suppression can be observed in spectroscopic measurements above the magnetic ordering temperature. We apply the criterion to high-resolution photoemission (UPS) measurements on $\text{CeCu}_{6-x}\text{Au}_x$ and conclude that the QPT in this system is dominated by the LQC scenario.

PACS numbers: 71.27.+a, 71.28.+d, 79.60.-i, 71.10.-w

1. Introduction

At a 2nd-order phase transition the characteristic time scale of the order parameter fluctuations diverges (critical slowing down), because the energy difference between the ordered and the disordered phases, i.e. the fluctuation energy ω_{fl} vanishes continuously at the transition. If the phase transition occurs at a finite critical temperature T_c , quantum fluctuations of the order parameter are always cut off by the temperature T , since $T \approx T_c > \omega_{fl}$, and the order parameter fluctuations are thermally excited, i.e. incoherent (dark shaded regions in Fig. 1 a), b)). In this sense, such a phase transition is classical. If, however, the transition is tuned to absolute zero temperature by a non-thermal control parameter, the system is at the critical point in a quantum coherent superposition of the degenerate ordered and disordered states, respectively. The transition is called a quantum phase transition (QPT). For reviews see [1, 2]. The excitation spectrum above this quantum critical state may be distinctly different from the excitations of either phase, the disordered and the ordered

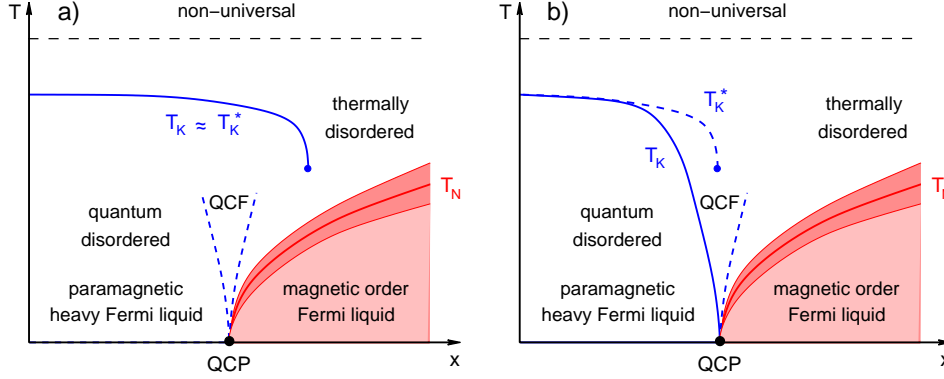


Figure 1. Generic phase diagrams of a magnetic QPT in a HF system, driven by an antiferromagnetic RKKY coupling (parametrized by a non-thermal control parameter x) for a) the HM and b) the LQC scenario. For both scenarios the predicted behavior of the spin screening scale, T_K , in the presence of quantum critical fluctuations (QCF) and as extracted from local Kondo ion spectra *without* lattice coherence or QCF, T_K^* , is also shown (see text for details). The maximum antiferromagnetic RKKY coupling, x_m , where single-ion Kondo screening terminates is marked by a \bullet .

one. Therefore, the physical properties are not only dominated by the quantum fluctuations between these phases at $T = 0$, but show also unusual temperature dependence essentially due to thermal excitation of the anomalous spectrum, so that the quantum critical behavior extends up to elevated temperatures (regions marked "QCF" in Fig. 1 a), b)).

In particular, in a number of heavy fermion (HF) compounds a magnetic phase transition may be suppressed to $T = 0$ by chemical composition, pressure or magnetic field. Two major scenarios are thinkable in such metallic systems.

In the first one, paramagnetic, heavy quasiparticles are formed due to the Kondo effect and subsequent lattice coherence. At the quantum critical point (QCP) the quasiparticle band then undergoes a spin density wave (SDW) instability, as described by the theory of Hertz [3] and Millis [4] (Hertz-Millis (HM) scenario). The instability can be caused by various types of residual spin exchange interactions. In this scenario the Landau Fermi liquid, albeit undergoing magnetic ordering, prevails, and the Kondo temperature T_K remains finite across the QPT.

In the second scenario, the Kondo effect and, hence, the very formation of heavy, fermionic quasiparticles are suppressed by magnetic coupling to the surrounding magnetic moments. In this case, both the bosonic order parameter fluctuations and the local fermionic excitations on the magnetic ions become critical at the QPT [5, 6]. This scenario has, therefore, been termed local quantum critical (LQC). In this case the system is in a more exotic, genuine many-body state which is not described by the Landau Fermi liquid paradigm.

Unambiguously identifying the quantum critical scenario from the low- T behavior, not to speak of predicting the scenario for a given system, has remained difficult. One reason for this is that neither the HM theory applied to heavy fermions, nor the description of the LQC scenario by an extended dynamical mean field theory [5] is complete, so that the precise critical behavior of either scenario is not known. While

the former theory pre-assumes fermionic quasiparticles with only bosonic, critical order parameter fluctuations, the latter neglects possible changes of the critical behavior due to non-trivial, spatially extended critical fluctuations. Motivated by our recent high-resolution ultraviolet (UPS) [7] and x-ray (XPS) [8] photoemission spectroscopy measurements of the Kondo resonance across the QPT in $\text{CeCu}_{6-x}\text{Au}_x$ at elevated T , we here put forward a criterion to predict the quantum critical scenario of a HF system from its high- T behavior around and above the single-ion Kondo temperature T_K . As seen below, this criterion derives from the fact that the Kondo screening breaks down completely when the dimensionless RKKY coupling y between Kondo ions exceeds a certain, universal strength y_m , even when critical fluctuations due to magnetic ordering do not play a role. This breakdown is related to the unstable fixed point of the two-impurity Kondo model which separates the Kondo screened and the inter-impurity (molecular) singlet ground states of this model [9]. However, in the present paper we explore and utilize its signatures at temperatures well above the lattice coherence temperature T_{coh} and the magnetic ordering or Néel temperature T_N .

In the following section 2 we present our calculations of the high-temperature signatures of the RKKY-induced Kondo breakdown using perturbative renormalization group as well as selfconsistent diagrammatic methods. In section 3 we briefly recollect the UPS results for $\text{CeCu}_{6-x}\text{Au}_x$ [7] and interpret them in terms of the high- T signatures of Kondo breakdown. Some general conclusions are drawn in section 4.

2. Theory for single-ion Kondo screening in a Kondo lattice

We consider a HF system described by the Kondo lattice model of local 4f spins 1/2 with the spin exchange coupling J and the density of states at the Fermi level, $N(0)$, for temperatures well above T_{coh} , T_N . In this regime controlled calculations of renormalized perturbation theory in terms of the single-impurity Kondo model are possible and can be directly compared to experiments [7]. In particular, the RKKY interaction of a given Kondo spin at site 0 with identical spins at the surrounding sites i can be treated as a perturbative correction to the local coupling J . The leading order direct and exchange corrections $\delta J^{(d)}$, $\delta J^{(ex)}$ are depicted diagrammatically in Fig. 2. As seen from the figure, these corrections involve the full dynamical impurity spin susceptibility (shaded bubbles) on the neighboring impurity sites i , $\chi_{4f}(T, 0) = (g_L \mu_B)^2 N(0) D_0 / (4\sqrt{T_K^{*2} + T^2})$, with the bare band width $D_0 \approx E_F$ and the Landé factor and the Bohr magneton g_L , μ_B , respectively [10]. In this expression we have named the Kondo temperature of this effective single-impurity problem T_K^* in order to distinguish it from the spin screening scale of the lattice problem, T_K . Summing over all lattice $i \neq 0$ one obtains [7],

$$\delta J^{(d)} = -y \frac{1}{4} J g_i^2 \frac{D_0}{\sqrt{T_K^{*2} + T^2}} \frac{1}{1 + (D/T_K^*)^2} \quad (1)$$

$$\delta J^{(ex)} = -y \frac{1}{4} J g_i^2 \left(\frac{3}{4} + \frac{T}{\sqrt{T_K^{*2} + T^2}} \right). \quad (2)$$

Here $g_i = N(0)J_i$ is the dimensionless, bare coupling on site $i \neq 0$, y is a dimensionless factor that describes the relation between the RKKY coupling strength and the Au content x . In the vicinity of the QPT the dependence is linear, $y = \alpha(x + x_0)$, with

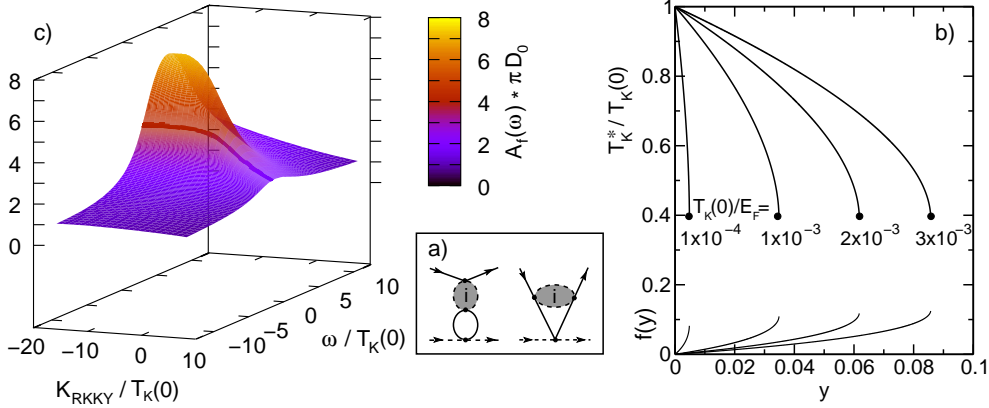


Figure 2. a) Leading order RKKY-induced corrections to the local spin exchange coupling. Solid and dashed lines represent conduction electron and impurity spin (pseudofermion) propagators, respectively. b) The single-impurity Kondo scale $T_K^*(y)$ with RKKY corrections to the local spin exchange coupling (Fig. 2 a)) is shown as a function of y for various values of the bare Kondo temperature $T_K(0)$. The effective perturbation parameter $f(y)$ is also shown. c) NCA result for the f spectral density on a single Kondo ion, including RKKY corrections (Fig. 2 a)) for $T = 2T_K(0)$. The steep collapse of the Kondo resonance for increasing, antiferromagnetic RKKY coupling K_{RKKY} is clearly seen.

adjustable parameters α and x_0 . As seen from Fig. 1 a), first diagram, $\chi_{4f}(T, \Omega)$ restricts the energy exchange between conduction electrons and local spin, i.e. the band cutoff D , to T_K^* . This is described by the last factor in Eq. (1) (soft cutoff). In $\delta J^{(ex)}$ (Fig. 1 b)) $\chi_{4f}(T, \Omega)$ restricts the conduction electron response to a shell of width T_K^* around the Fermi energy E_F , and suppresses $\delta J^{(ex)}$ compared to $\delta J^{(d)}$ by an overall factor of $\sqrt{T_K^{*2} + T^2}/D_0$, as seen in Eq. (2). The spin screening scale of this effective single-impurity problem, including RKKY corrections, can now be obtained as the energy scale where the perturbative renormalization group (RG) for the RKKY-corrected spin coupling (taken at $T = 0$) diverges. The one-loop RG equation reads,

$$\frac{dJ}{d \ln D} = -2N(0) \left[J + \delta J^{(d)}(D) + \delta J^{(ex)}(D) \right]^2. \quad (3)$$

Note that in this RG equation the bare band width D_0 and the couplings g_i on sites $i \neq 0$ are not renormalized, since this is already included in the full susceptibility χ_{4f} . The essential feature is that for $T = 0$ the direct RKKY correction $\delta J^{(d)}$, Eq. (1), is inversely proportional to the renormalized Kondo scale $T_K^*(y)$ itself via $\chi_{4f}(0, 0)$. The solution of Eq. (3) leads to a highly non-linear selfconsistency equation for $T_K^*(y)$,

$$\frac{T_K^*(y)}{T_K(0)} = \exp \left\{ - \left(\frac{1}{2g} + \ln 2 \right) \frac{f(u)}{1 - f(u)} \right\}, \quad (4)$$

with $g = N(0)J$, $f(u) = u - u^2/2$, $u = yg^2 D_0/[4T_K^*(y)]$. The single-ion Kondo scale without RKKY coupling is $T_K(0) = D_0 \exp[-1/2g]$. Fig. 2 b) shows solutions of Eq. (4) for various values of $T_K(0)$, together with the corresponding values of the effective perturbation parameter $f(y)$. It is seen that this RG treatment is perturbatively controlled in the sense that $f(y) \lesssim 0.1$, i.e. the exponent in Eq. (4) remains small for all solutions. Remarkably, a solution of Eq. (4) exists only up to

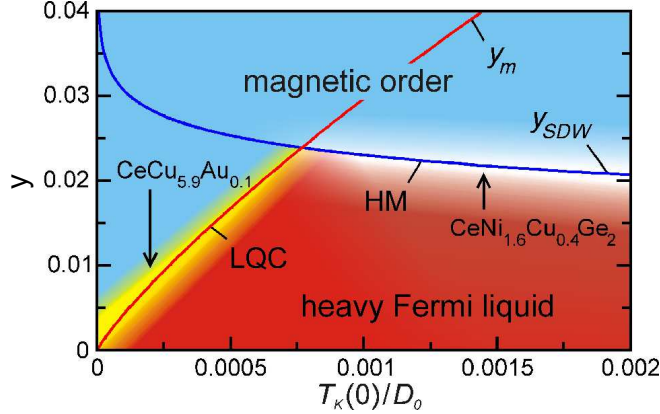


Figure 3. Schematic phase diagram of a HF system with a magnetic QPT in the $T_K(0)$ - y plane. The line denoted by y_m represents Eq. (5). At this line $T_K^*(y)$ undergoes an abrupt step, see text. The curve denoted by y_{SDW} marks, as an example, an SDW instability of the system. The magnetic phase transition, LQC- or HM-like, occurs at whichever of the two lines is lower. The arrows indicate estimates [22] for $T_K(0)/D_0$ for $\text{CeCu}_{6-x}\text{Au}_x$ and for $\text{CeNi}_{2-x}\text{Cu}_x\text{Ge}_2$.

a certain RKKY coupling strength y_m . For each value of the bare single-ion Kondo temperature, $\tau_K = T_K(0)/D_0$, y_m can be calculated as the point where the derivative $dT_K^*(y)/dy$ diverges [7],

$$y_m = 3.128 \tau_K (\ln \tau_K)^2 \left[2 - \ln \frac{\tau_K}{2} - \sqrt{\left(2 - \ln \frac{\tau_K}{2} \right)^2 - 4} \right]. \quad (5)$$

By rescaling y and $T_K^*(y)$ as y/y_m and $T_K^*(y)/T_K(0)$, respectively, all $T_K^*(y)$ curves collapse onto a single, universal curve, shown in the inset of Fig. 5. For $y > y_m$ the RG equation (3) does not diverge, i.e. the Kondo screening breaks down at this maximum RKKY coupling strength y_m , even if magnetic ordering does not occur. Therefore, the physical origin of the high- T criterion (5) is different from the well-known Doniach criterion [11] (which reads $T_K(0) \approx y_m N(0) J^2$), albeit it yields numerically similar values for y_m . According to Fig. 2 b) a sharp drop of T_K^* is predicted at $y = y_m$. As seen in Fig. 2 c), this breakdown of Kondo screening is signalled by a collapse of the Kondo resonance in the local 4f spectrum $A_f(\omega)$ of a single Kondo ion, as the antiferromagnetic RKKY coupling to neighboring Kondo ions is increased. Fig. 2 c) shows $A_f(\omega)$ as calculated for the two-impurity Anderson model within the non-crossing approximation (NCA) at $T = 2TK(0)$ [12]. For an efficient implementation of the NCA see [13]. Details of this calculations well as numerical renormalization group (NRG) studies of this problem will be published elsewhere. The described signatures should be directly observable in spectroscopic experiments at temperatures well above T_N , see section 3. We emphasize again that the Kondo breakdown occurs in any case, whether or not magnetic ordering sets in at low T .

Therefore, the theory predicts two quantum critical scenarios with distinctly different high- T signatures: (1) The heavy Fermi liquid has a magnetic, e.g., SDW instability at $T = 0$ for an RKKY parameter $y = y_{SDW} < y_m$, i.e., without breakdown of Kondo screening. In this case, $T_K^*(y)$, as extracted from high- T UPS spectra, is essentially constant across the QCP but does have a sharp drop at $y = y_m$ inside

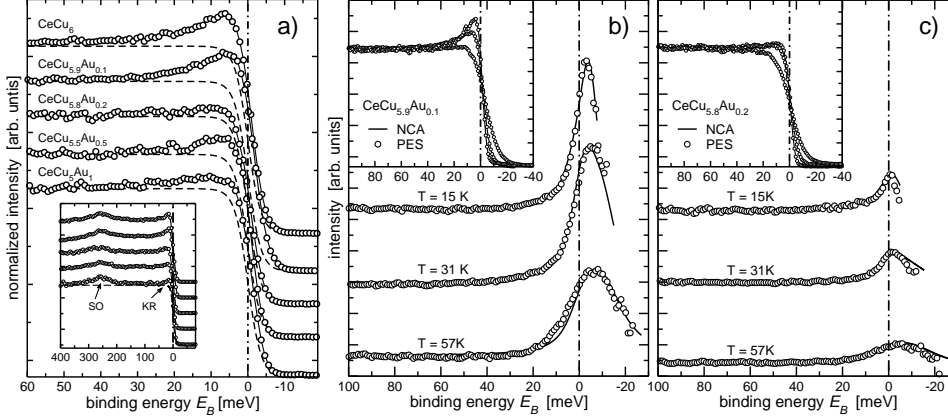


Figure 4. a) Near- E_F spectra of $\text{CeCu}_{6-x}\text{Au}_x$ for five different Au concentrations at $T = 15$ K. The dashed lines describe the resolution broadened FDD at $T = 15$ K. The inset shows a larger energy range including the spin-orbit (SO) satellite at $E_B \approx 260$ meV. For details of the experimental parameters see Ref. [7]. b) and c) show spectra for $x = 0.1$ and $x = 0.2$, respectively, divided by the FDD, at various T . The solid lines are single-impurity NCA fits. The insets in b) and c) show the corresponding raw data.

the region where magnetic ordering occurs at low T , see Fig. 1 a). This corresponds to the HM scenario. (2) Magnetic ordering does not occur for $y < y_m$. In this case the Kondo breakdown at $y = y_m$ implies that the residual local moments order at sufficiently low T , i.e. the magnetic QCP coincides with $y = y_m$. Quantum critical fluctuations (not considered in the present high- T theory) will suppress the actual Kondo screening scale T_K below the high- T estimate T_K^* , as shown in Fig. 1 b). This is the LQC scenario. These predictions are summarized in Fig. 3 as a phase diagram in terms of the bare Kondo scale $T_K(0)$ and the dimensionless RKKY coupling y [7].

3. High-resolution photoemission spectroscopy at elevated temperature

The theory described in the previous section should be applicable quite generally to HF systems with a magnetic QPT. Here we apply it to $\text{CeCu}_{6-x}\text{Au}_x$, where the Au content x is used to tune the RKKY interaction through the QPT at $x = x_c = 0.1$, and which is one of the best characterized HF compounds [14, 15, 16, 17, 18, 19, 20]. Our recent UPS measurements [7] on this compound at elevated T have actually motivated the theoretical study. Details of the sample preparation and measurement procedures can be found in [21, 22]. The UPS measurements were done at $T = 57$ K, 31 K and 15 K, i.e. well above $T_K(0) \approx 5$ K, T_{coh} and above the scale up to which quantum critical fluctuations extend in $\text{CeCu}_{6-x}\text{Au}_x$ [27]. Thus they record predominantly the local Ce 4f spectral density which is characterized by an effective *single-ion* Kondo scale T_K^* . This corresponds to the situation for which the calculations in section 2 were done. In Fig. 4 a) raw UPS Ce 4f spectra are displayed, showing the onset of the Kondo resonance. A sudden decrease of the Kondo spectral weight at or near the quantum critical concentration x_c can already be observed in these raw spectra. The states at energies of up to $5k_B T$ above the Fermi level can be made accessible by a now well-established procedure [21, 22] which involves dividing the raw UPS spectra

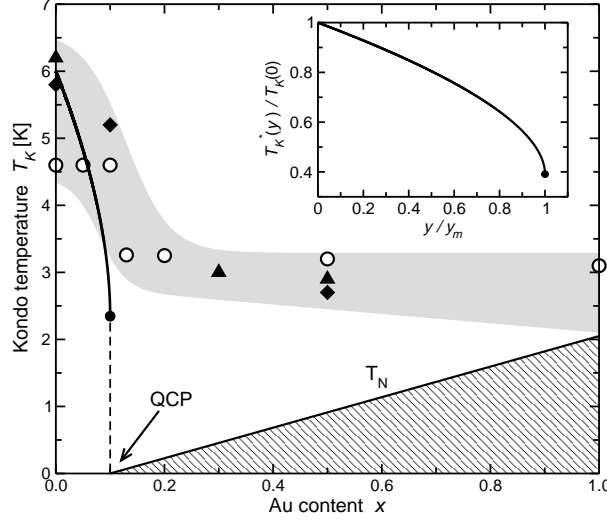


Figure 5. Dependence of the Kondo temperature T_K on the Au content x , as determined by UPS (open circles), specific heat [26] (triangles) and neutron scattering [19, 27] (diamonds). The error bars are approximately the width of the shaded area. The Néel temperature is labelled by T_N . The inset and the solid line in the main panel show the universal curve $T_K^*(y)/T_K(0)$ vs. y/y_m as given by Eq. (4).

by the Fermi-Dirac distribution (FDD). The Kondo resonance, which in $\text{CeCu}_{6-x}\text{Au}_x$ is located slightly above the Fermi level, then becomes clearly visible, see Fig. 4 b), c). These figures exhibit clearly the collapse of the Kondo spectral weight above as compared to below x_c . It is in qualitative accordance with the Kondo resonance collapse in the theoretical spectra at $T > T_K(0)$, Fig 2 c). To pinpoint the position of the Kondo breakdown more precisely, the single-ion Kondo temperature T_K^* was extracted from the experimental spectra for various x . To that end, we followed the procedure successfully applied to various Ce compounds in the past [23, 24, 25, 21, 22]: Using the non-crossing approximation (NCA) [13] the Ce 4*f* spectral function of the single-impurity Anderson model was calculated, including all crystal field and spin-orbit excitations. For each composition x the NCA spectra are broadened by the experimental resolution and fitted to the experimental data, using a single parameter set for all experimental T . The NCA spectra were then computationally extrapolated to $T \approx 0.1 T_K$, where T_K is extracted from the Kondo-peak half-width at half maximum (HWHM) of the NCA spectra. The results are shown in Fig. 5, with special emphasis on the region around x_c . Despite an uncertainty in T_K estimated by the width of the shaded area a sudden decrease of T_K^* as extracted from the experimental spectra is clearly visible. The fact that this Kondo breakdown occurs at (or very close to) the quantum critical concentration x_c strongly supports that the QPT in $\text{CeCu}_{6-x}\text{Au}_x$ follows the LQC scenario, as explained in section 2, and as was previously conjectured from neutron scattering experiments [27]. The finite Kondo scale for $x > x_c = 0.1$ results merely from the high- T onset of the Kondo resonance seen in Fig. 4 c) which is expected not to persist to low T .

4. Conclusion

The theoretical analysis predicts generally that an abrupt step of the Kondo screening scale extracted from high- T spectral data should occur in any HF compound with competing Kondo and RKKY interactions, as long as the single-ion Kondo screening scale is larger than the magnetic ordering temperature. Whether this distinct feature is located at the quantum critical control parameter value x_c or inside the magnetically ordered region constitutes a general high- T criterion to distinguish the LQC and HM scenarios. Moreover, this criterion allows to predict whether a given system should follow the HM or the LQC scenario, once estimates for the bare single-ion Kondo scale $T_K(0)$ and for dimensionless, critical coupling strength y_{SDW} for an SDW instability in that system are known. This is shown in Fig. 3 for the examples of $\text{CeCu}_{6-x}\text{Au}_x$ and $\text{CeNi}_{2-x}\text{Cu}_x\text{Ge}_2$. A systematical analysis of other HF compounds in this respect is in progress.

We would like to thank F. Assaad, L. Borda, S. Kirchner, and M. Vojta for fruitful discussions. This work was supported by DFG through Re 1469/4-3/4 (M.K., A.N., F.R.), SFB 608 (J.K.) and FOR 960 (H.v.L.).

References

- [1] v. Löhneysen H, Rosch A, Vojta M and Wölfle P 2007 *Rev. Mod. Phys.*, **79** 1015
- [2] Gegenwart P, Si Q and Steglich F 2008 *Nature Phys.* **4** 186
- [3] Hertz J A 1976 *Phys. Rev. B* **14** 1165
- [4] Millis A 1993 *Phys. Rev. B* **48** 7183
- [5] Si Q, Rabello S and Smith J L 2001 *Nature* **413** 804
- [6] Coleman P, Pépin C, Si Q and Ramazashvili R 2001 *J. Phys. Cond. Mat.* **13** R723
- [7] Klein M, Nuber A, Reinert F, Kroha J, Stockert O and v. Löhneysen H 2008 *Phys. Rev. Lett.* **101**, 266404
- [8] Klein M, Kroha J, v. Löhneysen H, Stockert O and Reinert F, 2009 *Phys. Rev. B* **79**, 07511
- [9] Jones B A and Varma C M 1987 *Phys. Rev. Lett.* **58**, 843
- [10] Andrei N, Furuya K and Löwenstein J H 1983 *Rev. Mod. Phys.* **55**, 331
- [11] Doniach S 1977 *Physica B & C* **91**, 231
- [12] Keiter H and Kimball J C 1971 *Int. J. Magn.* **1**, 233; Grewe N and Keiter H 1981 *Phys. Rev. B* **24**, 4420; Kuramoto Y 1984 *Z. Physik B* **53**, 37
- [13] Costi T A, Kroha J and Wölfle P 1996 *Phys. Rev. B* **53**, 1850
- [14] v. Löhneysen H, Pietrus T, Portisch G, Schlager H G, Schröder A, Sieck M and Trappmann T 1994 *Phys. Rev. Lett.* **72**, 3262
- [15] v. Löhneysen H 1996 *J. Phys. Cond. Mat.* **8**, 9689
- [16] v. Löhneysen H, Mock S, Neubert A, Pietrus T, Rosch A, Schröder A, Stockert O and Tutsch U 1998 *J. Magn. Mag. Mat.* **177–181**, 12
- [17] Stockert O, v. Löhneysen H, Rosch, A Pyka N and Loewenhaupt M 1998 *Phys. Rev. Lett.* **80**, 5627
- [18] v. Löhneysen H, Neubert A, Pietrus T, Schröder A, Stockert O, Tutsch U, Löwenhaupt M, Rosch A and Wölfle P 1994 *Eur. Phys. J. B* **5**, 447
- [19] Stroka B, Schröder A, Trappmann T, v. Löhneysen H, Loewenhaupt M and Severing A 1993 *Z. Phys. B* **90**, 155
- [20] Stockert O, Enderle M and v. Löhneysen H, 2007 *Phys. Rev. Lett.* **99**, 237203
- [21] Reinert F, Ehm D, Schmidt S, Nicolay G, Hüfner S and Kroha J 2001 *Phys. Rev. Lett.* **87**, 106401
- [22] Ehm D, Hüfner S, Reinert F, Kroha J, Wölfle P, Stockert O, Geibel C and v. Löhneysen H 2007 *Phys. Rev. B* **76**, 045117
- [23] Patthey F, Imer J-M, Schneider W-D, Beck H, Baer Y and Delley B 1990 *Phys. Rev. B* **42**, 8864
- [24] Garnier M, Breuer K, Purdie D, Hengsberger M and Baer Y 1997 *Phys. Rev. Lett.* **78**, 4172
- [25] Allen J et al. 2000 *J. Appl. Phys.* **87**, 6088
- [26] Schlager H G, Schröder A, Welsch M and v. Löhneysen H 1992 *J. Low Temp. Phys.* **90**, 181
- [27] Schröder A, Aepli G, Coldea R, Adams M, Stockert O, v. Löhneysen H, Bucher E, Ramazashvili R, and Coleman P 2000 *Nature* **407**, 351